International Journal of Pharmaceutics 657 (2024) 124197

Contents lists available at ScienceDirect

International Journal of Pharmaceutics

journal homepage: www.elsevier.com/locate/ijpharm

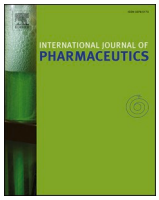

Combination of co-amorphization with SNEDDS outperforms Ofev® in the oral absorption of nintedanib

Tomoya Inoue [a,b], Seito Maehara [a], Masato Maruyama [a], Kazutaka Higaki [a,*]

[a] Department of Pharmaceutics, Faculty of Pharmaceutical Sciences, Okayama University, 1-1-1 Tsushima-naka, Kita-ku, Okayama 700-8530, Japan
[b] Formulation Research, Biopharmaceutical Research, Pharmaceutical Technology Division, Taiho Pharmaceutical Co., Ltd., 224-2 Ebisuno, Hiraishi, Kawauchi-cho, Tokushima 771-0194, Japan

ARTICLE INFO

Keywords:
Co-amorphous
Nintedanib
Ofev®
Brick dust
SNEDDS
Solubility
Oral absorption

ABSTRACT

Nintedanib (NTD), approved for the treatment of idiopathic pulmonary fibrosis and advanced non-small cell lung cancer, is one of brick dusts with high melting point. Although NTD has been marketed as Ofev®, a soft capsule of NTD ethanesulfonate (NTD-ESA) suspended in oil components, the oral bioavailability is quite low and highly variable. To improve the oral absorption behavior of NTD, we prepared SNEDDS formulation containing NTD-(+)-10-camphorsulfonic acid (CSA) complex with 2% HPMCP-50. CSA disrupted the high crystallinity of NTD-ESA and the formed complex, NTD-CSA, was found to be amorphous by DSC and XRPD. NTD-CSA provided solubilities in various vehicles much higher than NTD-ESA. Under the gastric luminal condition, NTD-CSA SNEDDS with or without 2% HPMCP-50 and NTD-CSA powder indicated very good dissolution of NTD from early time periods, while NTD was gradually dissolved until around 60 min from NTD-ESA and Ofev®. Under the small intestinal luminal condition, in contrast, both NTD-CSA SNEDDS formulations almost completely dissolved NTD throughout the experiments, while Ofev®, NTD-CSA, and NTD-ESA exhibited a very poor dissolution of NTD. In the in vivo absorption study, NTD-CSA SNEDDS with 2% HPMCP-50 significantly improved NTD absorption and reduced the inter-individual variation in oral absorption behavior compared with Ofev®.

1. Introduction

Nintedanib (NTD) is a potent tyrosine kinase inhibitor blocking the kinase activity of various receptors such as vascular endothelial growth factor receptor (VEGFR) 1–3, platelet-derived growth factor receptor (PDGFR)-α and -β, fibroblast growth factor receptor (FGFR) 1–3 (Hilberg et al., 2008; Roth et al., 2009) and non-receptor tyrosine kinases (RTKs), including Fms-like tyrosine-protein kinase 3 (FLT-3) and ret proto-oncogene (RET) (NDA review, FDA, 2014). Therefore, NTD was approved for the treatment of idiopathic pulmonary fibrosis (Package insert of Ofev®, 2022; Summary of product characteristics, Ofev®, 2018) and for the use in combination with docetaxel in patients with locally advanced, metastatic or recurrent non-small cell lung carcinoma (Summary of product characteristics, Ofev®, 2018). NTD has been marketed as Ofev®, which is the soft capsule of NTD ethanesulfonate (NTD-ESA) suspended in triglyceride, hard fat, lecithin, gelatin, glycerin, titanium oxide, red ferric oxide, and yellow ferric oxide (NDA review, FDA, 2014). The bioavailability (BA) of NTD after oral dosing of Ofev® was around 4.7% (Dallinger et al., 2016), for which the reasons were suggested to be the efflux by P-glycoprotein (P-gp) (Luedtke et al., 2018) and substantial first-pass metabolism via small intestine/liver (Summary of product characteristics, Ofev®, 2018). Since a high-fat meal tended to increase the oral absorption of NTD (Wind et al., 2019), the poor solubility of NTD would also be one of the reasons for its low BA. NTD-ESA is also classified into BCS class II or IV (Wind et al., 2019). Furthermore, a relatively large inter-individual variability in pharmacokinetic behavior as shown in coefficients of variation (CV) ranged from 46 to 83% is thought to be due to the variation in absorption process (Wind et al., 2019). Considering that the formulation type of Ofev® is an oil suspension, the oral absorption of NTD might be improved by some formulations that could increase the solubility of NTD. NTD-ESA is highly crystalline with 305°C of melting point (Roth et al., 2015 and Table 1) and its solubility in aqueous vehicle under neutral or basic pH and several lipoidal vehicles is quite low (Wind et al., 2019 and Table 2), indicating that NTD-ESA should be one of compounds called as “brick dust”.

Brick dust is highly crystalline with high crystal packing energy (Stella et al., 2007), possesses the melting point over 200°C (Sahbaz

* Corresponding author.
E-mail address: higaki@okayama-u.ac.jp (K. Higaki).

https://doi.org/10.1016/j.ijpharm.2024.124197
Received 3 October 2023; Received in revised form 4 April 2024; Accepted 1 May 2024
Available online 3 May 2024

et al., 2015), and is poorly soluble in both aqueous and lipoidal vehicles (Stella et al., 2007; Sahbaz et al., 2015). Since brick dusts are "at greatest risk of solid-state limitation to solubility" (Bergstrom et al., 2016), additional efforts should be required to prepare some dosage forms leading to the sufficient pharmacological effect. Although few attempts formulating compounds like brick dusts were reported until 2007 (Stella et al., 2007), trials to overcome the low solubility issue of brick dusts have recently increased as follows. The formation of lipophilic salt (Morgen et al., 2017) or ionic liquid (Serajuddin, 1999; Sahbaz et al., 2015) of active pharmaceutical ingredient (API) was reported for its utility and the prodrug strategy was also suggested to be beneficial to disrupt the high crystallinity of brick dust molecule (Stella et al., 2007). Particle size reduction, amorphization, lipid-based formulation (Nyamba et al., 2021), nanocrystal-silica-lipid particles (Meola et al., 2018), amorphous nanosuspension (Chougule et al., 2023), co-amorphization with an adequate co-former (Kasten et al., 2019; Aikawa et al., 2023) and phospholipid-based solid dispersion (Lale et al., 2024) were also applied for formulating brick dust-like drugs. Furthermore, it was recently suggested that the usage of ionic liquids as adjuvant components would efficiently enhance the solubility of poorly water-soluble API (Egorova et al., 2017). As for NTD, it has recently been reported that amorphous solid dispersion (Qin et al., 2022) and formation of lipid carrier (Zhu et al., 2020) improved the oral BA of NTD to some extent, compared with NTD-ESA. Lipid-based formulations have been used to improve oral absorption of poorly water-soluble drugs for many years (Holm et al., 2023). In the case of brick dusts, however, the limited lipid solubility in lipid-based formulations leads to incomplete dose loading on the formulations (Jadhav et al., 2024) and not necessarily to improved drug absorption (Koehl et al., 2019; Jadhav et al., 2024). Therefore, some approaches are needed to improve drug solubility in lipoidal components by utilizing amorphous drugs (Nora et al., 2022), lipophilic salts (Sahbaz et al., 2015; Sahbaz et al., 2017; Jadhav et al., 2024), and drug-phospholipid complexes (Huang et al., 2019; Jadhav et al., 2024). A dosing method such as chase dosing of lipid formulation have also been applied to overcome brick dust (Koehl et al., 2020).

We have recently reported that the complex formation with some counter ion resulted in the amorphization of a brick dust-like compound such as rebamipide (Okawa et al., 2021) and mebendazole (Sumimoto et al., 2022), and the co-amorphous complex of each compound extensively improved the solubility in water and various lipoidal vehicles. Although the oral administration of the co-amorphous complex powders did not lead to the improvement of BA, SNEDDS formulations containing the co-amorphous complex significantly improved the oral absorption of rebamipide or mebendazole. Furthermore, the addition of some polymer into the SNEDDS formulation led to the further improvement of BA for both brick-dust like compounds (Okawa et al., 2021; Sumimoto et al., 2022). Our previous results suggested that "the improvement of solubility by co-amorphization and the preparation of SNEDDS formulation with some polymer for the co-amorphous complex" would be a promising strategy to overcome the difficulty for preparing the formulations of brick dust-like compounds. In the current study, we aimed to improve the BA of NTD, a brick dust, by applying our strategy with (+)-10-camphorsulfonic acid (CSA) or 2-naphtalenesulfonic acid (NSA) as a counter ion, and successfully improved the solubility of NTD in various lipoidal vehicles by the co-amorphous formation with CSA, and improved the oral absorption of NTD by the SNEDDS formulation of the co-amorphous complex, NTD-CSA, compared with Ofev®, a marketed medicine of NTD-ESA.

Table 2
Solubilities of NTD-ESA in various vehicles.

Vehicles	Solubility (mg/mL of NTD)	Vehicles	Solubility (mg/mL of NTD)
Distilled water	4.72 ± 0.09	Olive oil	0.046 ± 0.006
pH3.9 acetate buffer	7.21 ± 0.13	Cremophor RH40	0.44 ± 0.08
pH6.5 FaSSIF	0.012 ± 0.000	Cremophor EL	0.33 ± 0.08
Ethanol	1.30 ± 0.39	Transcutol P	0.98 ± 0.57
Capryol 90	0.22 ± 0.06	SNEDDS vehicle [a)]	1.27 ± 0.23
Castor oil	0.048 ± 0.002		

Results are expressed as the mean ± S.D. of three experiments. [a)] Composition of SNEDDS vehicle is Capryol 90 : Cremophor EL : Transcutol P = 4 : 3 : 3 [Okawa et al., 2021; Sumimoto et al., 2022].

2. Materials and methods

2.1. Materials

Nintedanib ethanesulfonate (NTD-ESA) (Fig. 1 and Table 1) and Ofev® were kindly supplied by Towa Pharmaceutical Co., Ltd. (Kyoto, Japan). Ethanesulfonic acid (ESA), 2-naphtalenesulfonic acid (NSA), (+)-10-camphorsulfonic acid (CSA) (Fig. 1 and Table 1), and albendazole, an internal standard, were purchased from Tokyo Chemical Industry Co., Ltd. (Tokyo, Japan). HPMCP-50 was kindly supplied by Shin-Etsu Chemical Co., Ltd. (Tokyo). Transcutol P was obtained from Tokyo Chemical Industry Co., Ltd. Cremophor EL and Cremophor RH40 were obtained from Sigma Chemical Co. (St. Louis, MO, USA). Capryol 90 was kindly supplied from CBC Co., Ltd. (Tokyo). Olive oil and Castor oil were obtained from Nacalai Tesque, Inc. (Kyoto) and FUJIFILM Wako pure chemical Co. (Osaka, Japan), respectively. Other chemicals were analytical grade commercial products.

2.2. NTD-counter ion complex formation

NTD-ESA was used to form the complex of NTD with NSA or CSA and the complex formation was confirmed by increased solubility of NTD in ethanol with the addition of a counter ion as reported previously (Sumimoto et al., 2022). Briefly, several different amounts of each counter ion (NSA, 1 – 96 μmol; CSA, 17 – 86 μmol) were added into the ethanol containing an excessive amount of NTD-ESA and the mixture was vortexed for 1 min. Then, the supernatant obtained by centrifugation was filtered with the membrane filter (OD, 0.45 μm) and used for HPLC analysis of NTD.

2.3. Preparation of NTD-CSA complex powder

NTD-ESA and CSA were dissolved in distilled water at the molar ratio calculated based on the results obtained in Section 2.2 and vortex-mixed. Then, the solution was frozen at −80°C for 6 h, and lyophilized for 12 h by a freeze dryer (FDU-2100, EYELA, Tokyo) to obtain NTD-CSA powder. We confirmed that ESA was not detectable in ethanol

Table 1
Physicochemical properties of NTD-ESA and counter ions used for forming the complex with NTD.

Chemicals	Mw	Melting point (°C)	pKa	clogP	Chemical structures
Nintedanib (NTD)-Ethanesulfonate (ESA)	649.76	305	7.9	3.6	Fig. 1 (A)
Counter ions					
Ethanesulfonic acid (ESA)	110.13	−17.0	1.83	−1.89	Fig. 1 (B)
2-Naphtalenesulfonic acid hydrate (NSA)	208.2 (anhydrate)	124.0	0.27	0.529	Fig. 1 (C)
(+)-10-Camphorsulfonic acid (CSA)	232.29	200.0	1.17	−0.288	Fig. 1 (D)

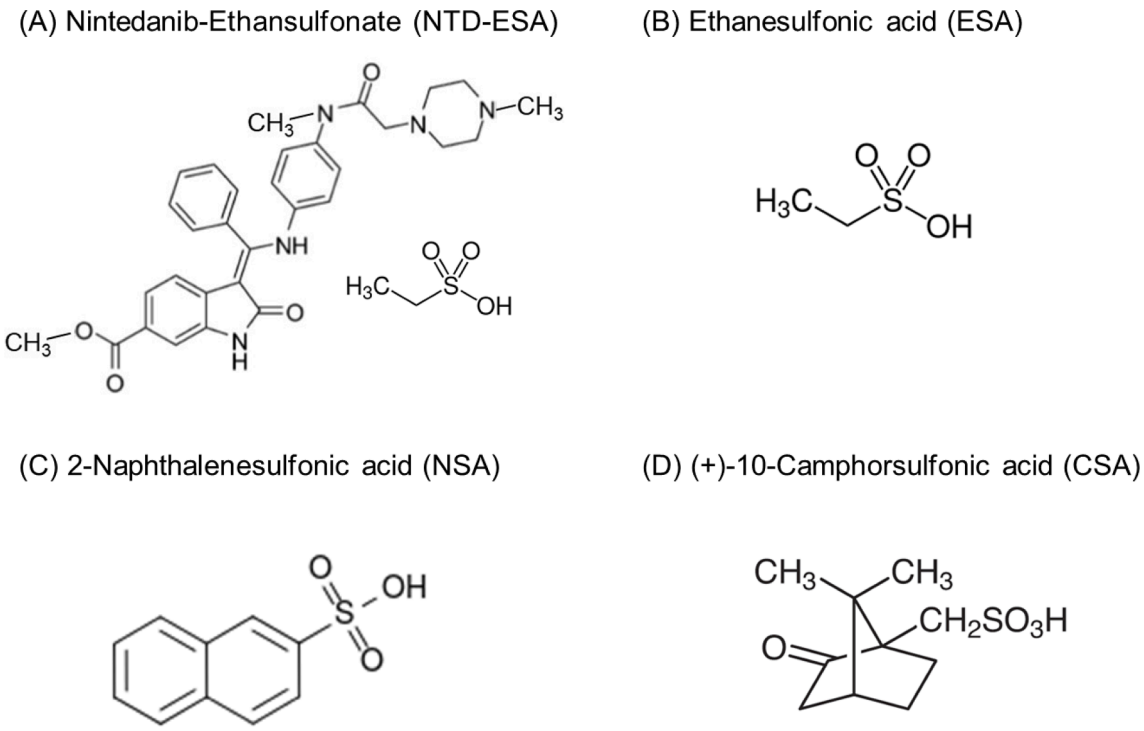

Fig. 1. Chemical structures of (A) NTD-ESA, (B) ESA, (C) NSA, and (D) CSA.

solution where NTD-CSA powder was dissolved.

2.4. Solubility determination

An excessive amount of NTD-ESA or NTD-CSA added into 1 mL or 1 g of various vehicles was shaken at 100 min^{-1} at 37°C for 48 h. Then, samples were centrifuged at 12,000 rpm for 10 min as reported previously (Sumimoto et al., 2022). The obtained supernatant was used for HPLC analysis of NTD.

2.5. Differential scanning calorimetry (DSC)

DSC curves were obtained with 2 mg of each sample placed in an aluminum pan (Φ 6 × 1.5 mm) of DSC-50 (Shimadzu, Kyoto). The heating rate was 5°C/min from 30 to 330°C.

2.6. X-ray powder diffraction (XRPD)

XRPD was performed with RINT-TTR III (Rigaku Co., Tokyo). The Cu anode X-ray source was operated under a voltage of 50 kV and current of 250 mA. The scanning rate was 10°/min over a 2θ range of 5 to 60° and with a sampling interval of 0.02°.

2.7. SNEDDS vehicle

The solubilities of NTD-ESA (Table 2) and NTD-CSA (Table 3) in each excipient indicated that Capryol 90 and Transcutol P should be selected as an oil component and a cosolvent of SNEDDS, respectively. Furthermore, since our previous results revealed that Capryol 90 : Cremophor EL : Transcutol P = 4 : 3 : 3 (w/w/w) with or without HPMCP-50 provided a larger area of nanoemulsion formation in the psuedo-ternary phase diagrams and the good performance for brick dust-like drugs in in vitro and in vivo studies (Okawa et al., 2021; Sumimoto et al., 2022), the composition was chosen to prepare the SNEDDS vehicle. To estimate the improvement of solubility of NTD in SNEDDS by each NTD-counter ion complex, SNEDDS vehicle was prepared first and then, each complex was put into the SNEDDS vehicle and its solubility was examined.

2.8. Measurement of particle sizes of nanoemulsion droplets

Size distribution of nanoemulsion droplets was determined by the dynamic light scattering method (Zetasizer Nano ZS, Malvern Instruments, Ltd., Worcestershire, UK) at 25°C. Nanoemulsion was prepared following the dosing condition or oral absorption study described below. The laser was operated at 633 nm and the detector position was at 173°.

Table 3
Solubilities of NTD-CSA in various vehicles.

Vehicles	Solubility (mg/mL of NTD)	Ratio to NTD-ESA in solubility	Vehicles	Solubility (mg/mL of NTD)	Ratio to NTD-ESA in solubility
Distilled water	97.29 ± 5.14	20.7	Olive oil	0.021 ± 0.002	0.5
pH3.9 acetate buffer	104.46 ± 1.39	14.5	Cremophor RH40	2.05 ± 0.52	4.7
pH6.5 FaSSIF	0.044 ± 0.001	3.7	Cremophor EL	1.51 ± 0.26	4.6
Ethanol	45.15 ± 3.92	34.7	Transcutol P	26.34 ± 3.75	26.8
Capryol 90	22.62 ± 4.36	102.8	SNEDDS vehicle [a)]	19.05 ± 1.03	15.0
Castor oil	0.59 ± 0.07	12.3			

Results are expressed as the mean ± S.D. of three experiments. [a)] Composition of SNEDDS vehicle is Capryol 90 : Cremophor EL : Transcutol P = 4 : 3 : 3 [Okawa et al., 2021; Sumimoto et al., 2022].

2.9. Dissolution of NTD-ESA and NTD-CSA in SNEDDS vehicle

NTD-ESA (ca 2 mg as NTD) or NTD-CSA (ca 35 mg or 18 mg as NTD) was compulsorily dissolved in 1 g SNEDDS vehicle by sonication. Then, the SNEDDS vehicle dissolving NTD-ESA or NTD-CSA was kept at 37°C for 28 days. Fifty μL of supernatant was periodically sampled and centrifuged at 12,000 rpm for 10 min. The obtained supernatant was used for HPLC analysis of NTD or CSA.

2.10. In vitro dissolution study

According to the dosing condition of oral absorption study, each preparation containing NTD at 15 mg was dispersed into 3.2 mL of aqueous vehicle (pH3.9 acetate buffer (McConnell et al., 2008) or pH6.5 FaSSIF) and stirred at 50 rpm at 37°C for 90 min or 240 min. The supernatant periodically sampled was filtered through 0.45 μm membrane filter, used for determining NTD dissolved directly in buffer and dispersed as nanoemulsion and/or micelles in buffer.

On the other hand, for determining only NTD dissolved directly in buffer, an aliquot of samples periodically taken was ultrafiltrated by Amicon Ultra (UFC501096, MWCO 10 kDa, Merk KGaA, Darmstadt, Germany) at 10,000×g for 10 min to obtain the samples for analysis.

2.11. Solvent shift study

NTD-CSA in good solvent (methanol) was transferred to poor solvent (pH6.5 FaSSIF) (Yamashita et al., 2011) as follows. NTD-CSA was dissolved in methanol at 10 mg/mL with or without HPMCP-50 of 25 mg/mL. Then, 900 μL of pH6.5 FaSSIF was added to 100 μL of NTD-CSA methanol solution. The obtained mixture was shaken at 100 min^{-1} at 37°C for 0.5, 1 and 2 h. A sample obtained at each time was centrifuged at 12,000 rpm for 10 min and the obtained supernatant was used for HPLC analysis of NTD.

2.12. Oral absorption study

Our investigation utilizing animals was carried out after approval by the Animal Care and Use Committee of Okayama University and in accordance with the "Principles of Laboratory Animal Care (NIH publication #85–23)". Male Wistar rats weighing 254.2 ± 19.5 g (Charles River Laboratories Japan, Yokohama, Kanagawa, Japan) were fasted for 24 h prior to and during the experiment, but were allowed free access to water.

One day before the study, rats were prepared with a cannulation of jugular vein for blood sampling under anesthesia. NTD-counter ion complex powders or Ofev® were administered in an HPMC mini-capsule (Qualicaps, Nara, Japan) at 30 mg as NTD/kg. SNEDDS preparation was intragastrically administered with an animal feeding needle (18G-50, Natsume Seisakusho Co., Ltd., Tokyo) at 30 mg as NTD/2 g SNEDDS/kg. After oral administration of drug, water was immediately ingested to the rat with the animal feeding needle at 6.4 mL/kg. Thirty mg as NTD/kg rat corresponds to ca 300 mg/60 kg human (FDA, Guidance for industry, 2005), which is a recommended maximum daily dose (150 mg × 2) (Package insert of Ofev®, 2022). The dosed rats were allowed to move freely and were given free access to water after 4 h of administration. Blood samples, approximately 300 μL, were taken from the cannulated jugular vein at 0.5, 1, 2, 4, 6, 8, 12, and 24 h. Plasma obtained by centrifugation was deproteinized by acetonitrile and the resulting supernatant was used for HPLC analysis of NTD.

2.13. Analytical methods

The HPLC system was used for the analysis of NTD and CSA. A model SPD-20A (Shimadzu) was set at 290 nm for detection of NTD and CSA. A mobile phase (50 mM $(NH_4)_2SO_4$: methanol = 33 : 67 for in vitro sample or 38 : 62 for plasma sample) was delivered at 1.0 mL/min with a model LC-20AT pump (Shimadzu) at room temperature. Inertsil ODS-3 (250 × 4.6 mm, i.d., GL-Science, Tokyo) was used as a separation column. The injection of samples was performed with a model SIL-20A auto sampler (Shimadzu). The standard curves for NTD from 1 to 40 μg/mL provided the coefficient of variation (CV) between 1.73 and 11.7%. The standard curves of CSA from 1 to 40 μg/mL revealed the CV values between 0.99 and 9.30%. The correlation coefficients (r) were over 0.999. For plasma samples, the standard curves for NTD from 0.1 to 2 μg/mL indicated the CV values between 3.96 and 23.7% and the r values over 0.999. Limit of quantitation was the lowest value of each standard curve for NTD described above.

2.14. Pharmacokinetic analysis

The area under the plasma concentration – time curve, AUC, from 0 to 24 h was calculated following the trapezoidal rule. C_{max}, a maximum concentration, was the highest concentration observed and T_{max} was a time to reach C_{max}. The CV values for T_{max}, C_{max}, and AUC were calculated to estimate the variation of absorption kinetics for each formulation.

2.15. Statistical analysis

Analysis of variance (ANOVA) was utilized to test the statistical significance of differences among groups. Then, Student's *t*-test or Tukey's test was utilized to evaluate the statistical significance in the differences of the means.

3. Results and discussion

3.1. Formation of NTD-CSA and determination of the solubility in various vehicles

Since Ofev® has been marketed as a soft capsule of oil suspension of NTD-ESA (NDA review, FDA, 2014), we, first, examined the solubility of NTD-ESA in various aqueous and lipoidal vehicles (Table 2). Milligram-order solubilities were recognized for distilled water, pH3.9 acetate buffer and ethanol, but the solubility in pH6.5 FaSSIF was found to be only 12 μg/mL, indicating the difficulty in its dissolution in the small intestinal lumen. Furthermore, the solubilities in various lipoidal vehicles were found to be less than 1 mg/mL, convincing that Ofev® should be an oil suspension.

Next, the formation of the complex of NTD with NSA or CSA was examined in ethanol. When the added counter ion disrupts the high crystallinity of a brick dust, the solubility extensively increases over the solubility of brick dust crystalline in ethanol (Okawa et al., 2021; Sumimoto et al., 2022). As shown in Fig. 2 (A), NSA increased the solubility of NTD until around 20 μmol/mL where NTD-NSA was formed at 1 : 1 molar ratio, but thereafter the solubility fell down to ca 12 μmol/mL. Since the solubility of NTD-ESA is 2.41 μmol/mL, NSA improved the solubility of NTD, but the result indicated the interaction of NTD with NSA should be limited and NSA was not able to be replaced with ESA efficiently. In contrast, Fig. 2 (B) clearly indicated that CSA increased the solubility of NTD proportionally as CSA amount increased and the complex was found to be formed at the molar ratio of NTD to CSA, 100 : 107. Furthermore, ESA was not detectable by HPLC in the ethanol solution dissolving NTD-CSA powder, suggesting that ESA would have been almost completely replaced with CSA in forming the complex with NTD. Then, NTD-CSA complex was prepared at the molar ratio 100 : 107 for further studies.

Then, the solubilities of NTD-CSA were examined in various aqueous and lipoidal vehicles (Table 3). NTD-CSA extensively improved the solubility of NTD in distilled water or pH3.9 acetate buffer. The solubility in pH6.5 FaSSIF, although still very low, also increased 3.7 times compared to that by NTD-ESA. As for the lipoidal vehicles, NTD solubility was largely improved in Capryol 90 and Transcutol P, and

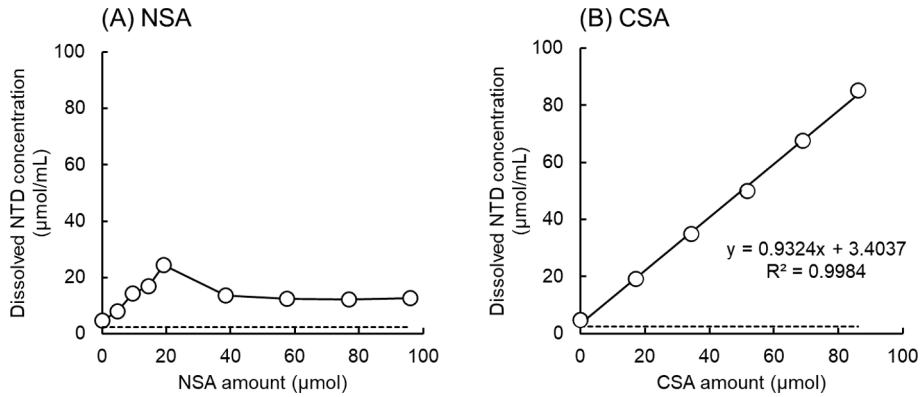

Fig. 2. Formation of NTD-NSA (A) or NTD-CSA (B) complex in ethanol. Results are expressed as the mean with S.D. bar of three experiments. S.D. bar was hidden behind the symbol. Dotted lines mean the solubility of NTD-ESA in ethanol (2.41 μmol/mL). (A) Until 20 μmol of NSA, NTD-NSA was formed at 1 : 1 molar ratio based on the linear regression line ($y = 1.0018x + 3.9953$, $R^2 = 0.9767$) (B) The molar ratio of NTD to CSA in the complex was calculated to be 100 : 107 based on the linear regression line ($y = 0.9324x + 3.4037$, $R^2 = 0.9984$).

therefore, the solubility in SNEDDS vehicle was also 15 times higher than that by NTD-ESA.

3.2. Characterization of solid state of NTD-CSA complex

The solid states of NTD-CSA and NTD-ESA were examined by DSC (Fig. 3 (A)) and XRPD (Fig. 3 (B)). NTD-ESA provided a large endothermic peak around 300°C in DSC thermogram and many sharp diffraction peaks in XRPD pattern, which are very similar with those reported (Zhu et al., 2020; Qin et al., 2022). In our previous study (Sumimoto et al., 2022), ESA formed the co-amorphous complex with mebendazole. However, NTD-ESA was confirmed to be crystalline with high melting point (Fig. 3). In contrast, both DSC and XRPD charts revealed a hallo pattern for NTD-CSA (Fig. 3 (A) and (B)), clearly indicating that NTD-CSA should be amorphous. The reason why only CSA has disrupted the high crystallinity of NTD-ESA would be as follows. Since the planarity and/or symmetry is considered to be an issue to be overcome to enhance the solubility of brick dust-like drugs (Ishikawa and Hashimoto, 2011), the steric structure of CSA as shown in Fig. 1 (D) would efficiently have disrupted the crystal packing of NTD-ESA and would have been stably co-amorphized with NTD.

3.3. Maintenance of supersaturation by HPMCP-50

As a polymer to maintain the supersaturation of NTD, HPMCP-50 was selected and examined by solvent shift method, because HPMCP-50 kept the highest concentration of mebendazole, a basic drug, among 10 polymers and gave the sustained release property to the SNEDDS formulation of mebendazole-CSA complex (Sumimoto et al., 2022). As shown in Fig. 4, HPMCP-50 was able to maintain NTD concentrations around five times higher than those without HPMCP-50 for 2 h, suggesting its possible usage as a precipitation inhibitor.

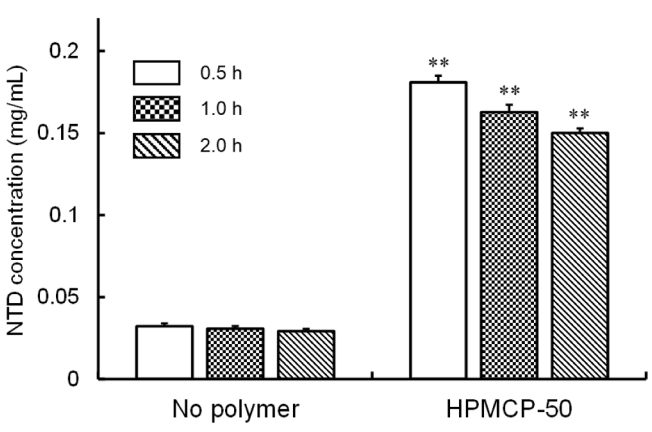

Fig. 4. Effect of HPMCP-50 on the solubility of NTD-CSA in solvent shift from methanol to pH6.5 FaSSIF. Results are expressed as the mean with S.D. bars of three experiments. **, $p < 0.01$ compared with no polymer at each time point.

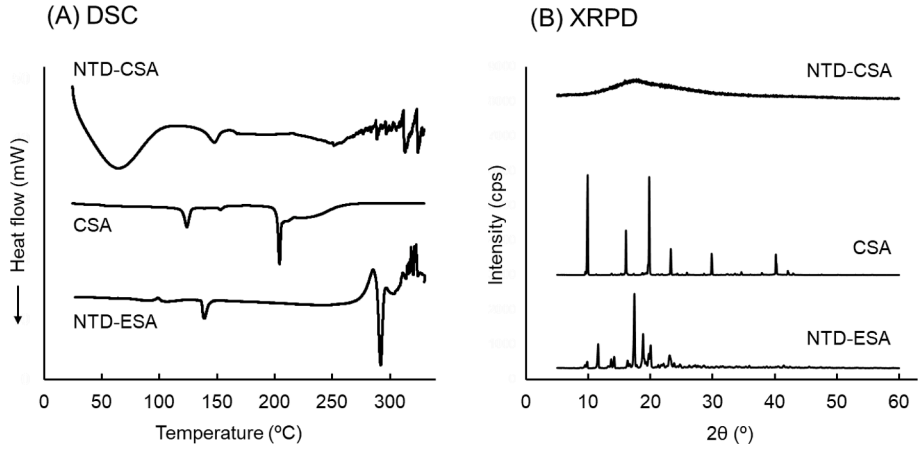

Fig. 3. Differential scanning calorimetry (DSC) thermograms (A) and X-ray powder diffraction (XRPD) patterns (B) of NTD-CSA, CSA, and NTD-ESA.

3.4. Dissolution and stability of NTD-CSA in SNEDDS vehicle

The dissolution and stability of NTD-CSA in SNEDDS vehicle (Capryol 90 : Cremophr EL : Transcutol P = 4 : 3 : 3, w/w/w) was examined (Fig. 5 (A)). In the case of loading dose 34.80 (± 2.69) mg as NTD/g SNEDDS, the dissolved concentration of NTD decreased and reached around 20 mg/g SNEDDS. On the other hand, the loaded NTD was almost completely dissolved until the end of study in the case of 18 mg (17.96 ± 0.64) as NTD/g SNEDDS. As for SNEDDS with 2% HPMCP-50 (loading dose, 20.15 ± 0.59 mg as NTD/g SNEDDS), although the final concentration was slightly lower than the initial value (17.16 ± 0.92 mg/g SNEDDS, not significant compared with the initial value), the concentration was maintained around the solubility of NTD in SNEDDS vehicle for NTD-CSA (Table 3). On the other hand, around 2 mg NTD/g SNEDDS was maintained for NTD-ESA (2.34 ± 0.18 mg as NTD/g SNEDDS) after dissolved by sonication. Fig. 5 (B) indicated fractions of NTD or CSA dissolved in SNEDDS vehicle for 28 days for NTD-CSA. The values for NTD and CSA were very similar throughout the experiment, indicating that both molecules should be dissolved together in SNEDDS vehicle. A slight discrepancy was observed between NTD and CSA in the case of 2% HPMCP-50 SNEDDS, but this could be due to the overestimation of the values of fraction dissolved for CSA.

The observation that the dissolution behavior of API into SNEDDS vehicle was consistent with that of counter ion (Fig. 5 (B)) was a situation as in the case of mebendazole and the three counter ions in the previous report (Sumimoto et al., 2022). These results suggest that NTD was dissolved into SNEDDS vehicle as a complex with CSA, which is reasonable considering that the solubility of NTD in SNEDDS vehicle was increased by forming the complex with CSA (Fig. 2 (B) and Tables 2 and 3). However, even in the case of NTD-CSA, NTD that dissolved above the solubility could not be maintained in a dissolved state (Fig. 5), and this was also the case for mebendazole-counter ion complexes (Sumimoto et al., 2022). Therefore, adequate doses causing API concentrations less than the solubility in SNEDDS vehicle would be able stably to maintain API dissolved in SNEDDS vehicle at least for approximately 1 month at 37°C for the cases of NTD and mebendazole (Sumimoto et al., 2022). Of course, further detailed stability analysis for every ingredient used and possible chemical degradation of APIs will be required to bring this formulation to market.

3.5. Dissolution of NTD and CSA from NTD-CSA SNEDDS formulations

Considering the capacity and stability of NTD dissolution in SNEDDS (Fig. 5), 15 mg NTD/g SNEDDS-loaded NTD-CSA SNEDDS formulations were prepared and examined in the in vitro dissolution studies. As shown in Fig. 6 (A), NTD was almost completely dissolved within 90 min for all preparations including NTD-ESA powders under gastric luminal condition. It would be due to a relatively high solubility of NTD-ESA in pH3.9 acetate buffer (Table 2), but the dissolution – time profile was clearly different between preparations for NTD-CSA and NTD-ESA. NTD-CSA preparations including powders indicated the very rapid dissolution of NTD and the maintenance of the highest concentration throughout the study, while NTD-ESA preparations including Ofev® indicated the gradual dissolution of NTD. Fig. 6 (B) indicated that the dissolution – time profiles of CSA were very similar to those of NTD of each corresponding preparation for NTD-CSA preparations.

Under the small intestinal luminal condition, only NTD-CSA SNEDDS formulations indicated almost complete dissolution of NTD from the beginning to the end of the experiment, while other preparations including NTD-CSA powder and Ofev® provided very low dissolution of NTD (Fig. 7 (A)). The inset of Fig. 7 (A) for NTD-CSA powder, NTD-ESA, and Ofev®, indicated that NTD-CSA powder improved the dissolution of NTD transiently around 10 times larger compared with NTD-ESA powder or Ofev®. However, the precipitation was promoted very rapidly because the degree of supersaturation was around 2 times larger for NTD-CSA (12.0; 0.53 mg/mL(=12% in Fig. 7(A))/0.044 mg/mL (Table 3)) than NTD-ESA (5.3; 0.063 mg/mL(=1.3%, Fig. 7(A))/0.012 mg/mL (Table 2)). It is well known that the nucleation rate is highly dependent on the degree of supersaturation (Brouwers et al., 2009). Furthermore, a "surface precipitation", very prevalent for soluble salts of poorly water-soluble chemicals (Hawley and Morozowich, 2010), might also have facilitated the precipitation of NTD for NTD-CSA. Fig. 7 (B) revealed that CSA was also almost completely dissolved throughout the study for both SNEDDS preparations. In addition, CSA was dissolved very rapidly to very large extent for NTD-CSA powder as well. Considering these results, it is suggested that NTD-CSA released from nanoemulsion droplets and/or micelles would be dissociated and then CSA would be dissolved, but NTD would precipitate based on its own solubility. Therefore, most of NTD would be dissolved in nanoemulsion

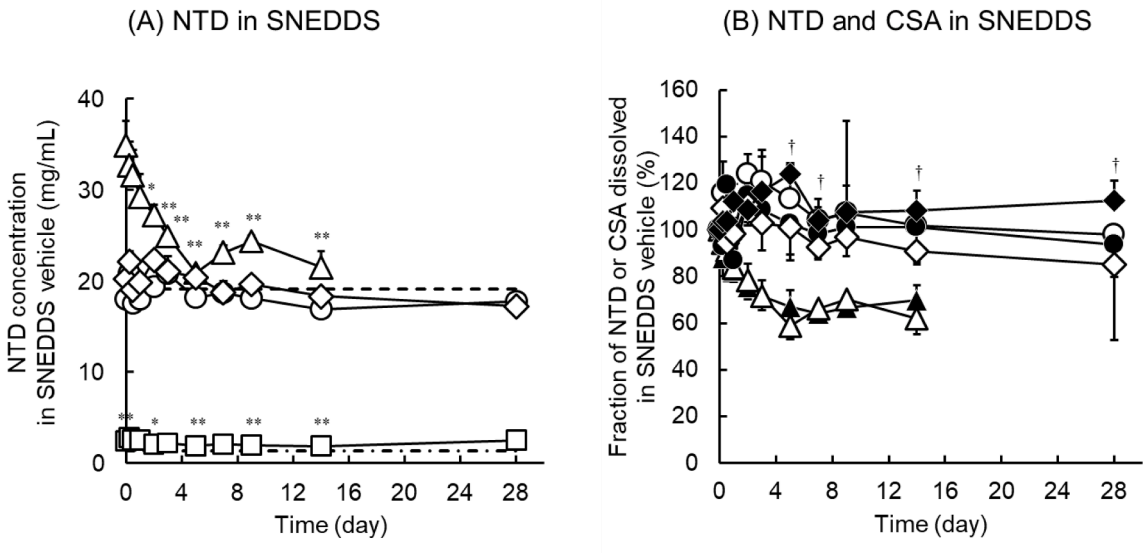

Fig. 5. Solubilizing stability of NTD-CSA in SNEDDS vehicle (A) and dissolution – time profiles of NTD or CSA in SNEDDS vehicle (B). Results are expressed as the mean with S.D. bars of three experiments. (A) **, $p < 0.01$; *, $p < 0.05$ compared with the value at day 0 for each formulation. (B) †, $p < 0.05$ compared with each corresponding value of NTD at each time point. Keys: △, NTD-CSA 40 mg/g SNEDDS; ○, NTD-CSA 18 mg/g SNEDDS; ◇, NTD-CSA 18 mg/g 2% HPMCP-50 SNEDDS; □, NTD-ESA 2 mg/g SNEDDS. Open and closed symbols mean NTD and CSA, respectively. Dotted line, NTD solubility from NTD-CSA in SNEDDS vehicle. Single-pointed line, NTD solubility from NTD-ESA in SNEDDS vehicle.

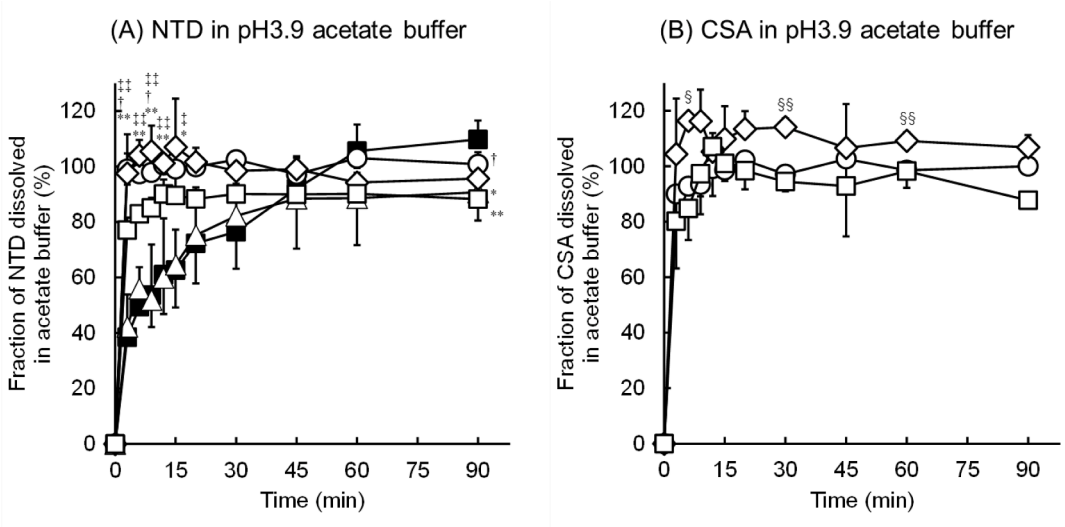

Fig. 6. Dissolution profile of NTD (A) and CSA (B) from each formulation under gastric luminal condition (pH3.9 acetate buffer). Results are expressed as the mean with S.D. bars of three experiments. (A) **, $p < 0.01$; *, $p < 0.05$ compared with NTD-ESA at each time point. †, $p < 0.05$ compared with NTD-CSA at each time point. ‡‡, $p < 0.01$; ‡, $p < 0.05$ compared with Ofev® at each time point. (B) §§, $p < 0.01$; §, $p < 0.05$ compared with fraction of dissolved NTD for each corresponding formulation at each time point shown in the panel (A). Keys: ■, NTD-ESA powder; □, NTD-CSA powder; △, Ofev®; ○, NTD-CSA SNEDDS; ◇, 2% HPMCP-50 NTD-CSA SNEDDS.

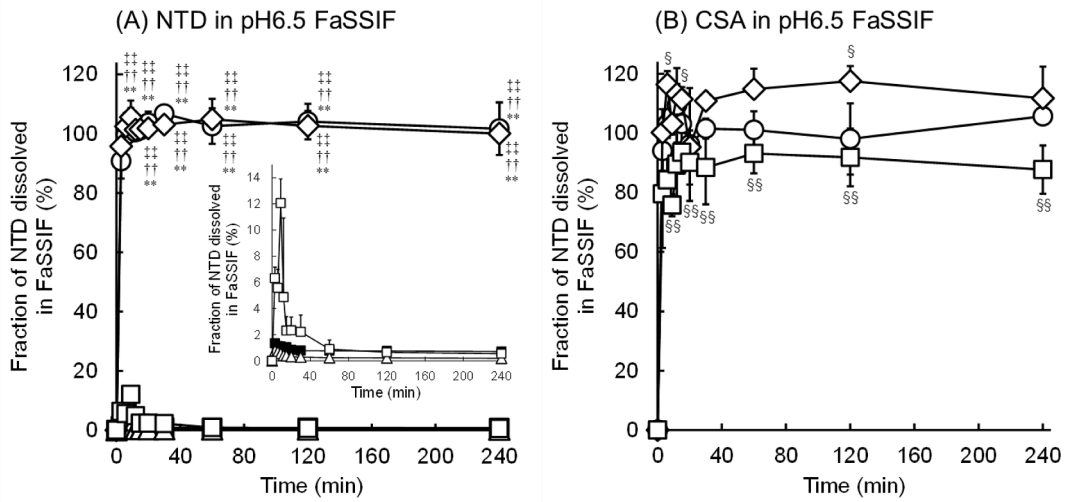

Fig. 7. Dissolution profile of NTD (A) and CSA (B) from each formulation under intestinal luminal condition (pH6.5 FaSSIF). Results are expressed as the mean with S.D. bars of three experiments. (A) Fractions of dissolved NTD less than 20% were shown in the inset graph. **, $p < 0.01$ compared with NTD-ESA at each time point. ††, $p < 0.01$ compared with NTD-CSA at each time point. ‡‡, $p < 0.01$ compared with Ofev® at each time point. (B) §§, $p < 0.01$; §, $p < 0.05$ compared with fraction of dissolved NTD for each corresponding formulation at each time point shown in the panel (A). Keys: ■, NTD-ESA powder; □, NTD-CSA powder; △, Ofev®; ○, NTD-CSA SNEDDS; ◇, 2% HPMCP-50 NTD-CSA SNEDDS.

droplets and/or micelles together with CSA under the small intestinal luminal condition.

On the other hand, since Fig. 6 (A) and 7 (A) revealed that NTD was rapidly dissolved at pH3.9, and poorly dissolved in pH6.5 FaSSIF, respectively, from NTD-CSA powders, NTD-CSA released from nanoemulsion droplets and/or micelles in nanoemulsion can also be dissolved in the acetate buffer to large extent, but not in pH6.5 FaSSIF. Furthermore, HPMCP-50, which can sustain the release of drugs dissolved in the nanoemulsion droplets by increasing the viscosity within the nanoemulsion droplets (Sumimoto et al., 2022), is substantially insoluble in the acidic aqueous vehicle, but soluble in neutral and basic aqueous vehicles (Home page of Shin-Etsu Chemical Co., Ltd.) since its pKa is 4.32 (Hiew et al., 2022). These characteristics of NTD-CSA and HPMCP-50 suggest that the release sustainability would be different, and thereby the distribution of NTD dissolved in the buffers (i.e., in the nanoemulsion droplets and/or micelles, directly in the aqueous phase) would be different between the two luminal conditions, although NTD was almost completely dissolved from SNEDDS formulations under both the two conditions (Figs. 6 and 7).

Then, the concentrations of NTD dissolved directly in pH3.9 buffer and pH6.5 FaSSIF were determined after separated from nanoemulsion droplets and/or micelles by ultrafiltration (Fig. 8). As for NTD-CSA SNEDDS without HPMCP-50, NTD concentrations dissolved directly in the aqueous phase were around 3.4 times higher in pH3.9 buffer than those in pH6.5 FaSSIF, where mean values throughout the experiments were 667.2 ± 133.4 μg/mL in pH3.9 acetate buffer and 196.8 ± 33.5 μg/mL in pH6.5 FaSSIF (vs. pH3.9, $p < 0.001$). In the case of NTD-CSA SNEDDS with 2% HPMCP-50, NTD concentrations in pH3.9 buffer and

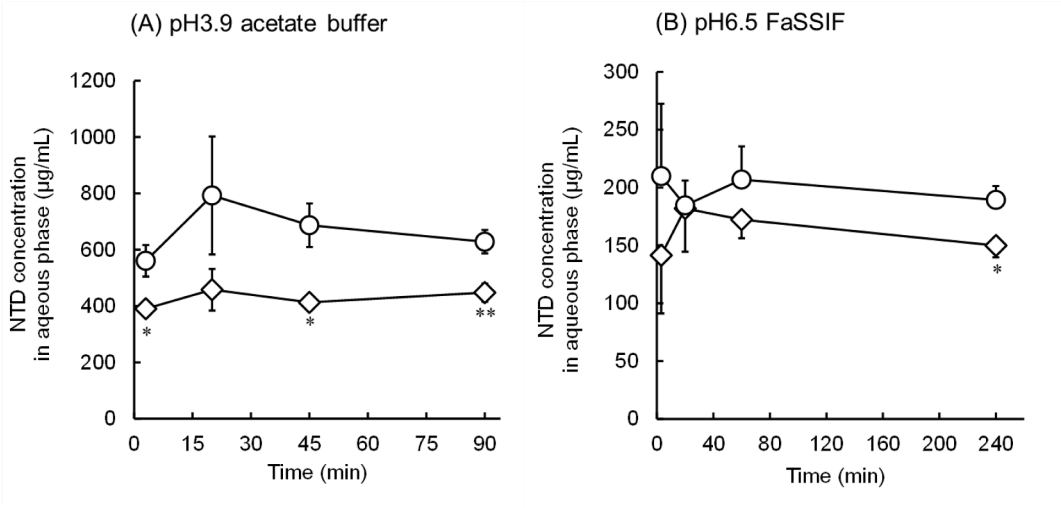

Fig. 8. NTD concentrations dissolved directly in the aqueous phase of NTD-CSA SNEDDS preparations under gastric (A) or intestinal (B) luminal condition. Results are expressed as the mean with S.D. bars of three experiments. **, $p < 0.01$; *, $p < 0.05$ compared with SNEDDS without HPMCP-50 at each time point. Keys: ○, NTD-CSA SNEDDS; ◇, 2% HPMCP-50 NTD-CSA SNEDDS.

pH6.5 FaSSIF were 429.7 ± 42.4 μg/mL and 162.6 ± 29.1 μg/mL (vs. pH3.9, $p < 0.001$), respectively. The results also clearly indicated that HPMCP-50 significantly suppressed the release of NTD from the nanoemulsion droplets and/or micelles in both buffers and that the suppressing effect was stronger in pH3.9 buffer (with/without HPMCP-50 ratio in NTD concentration, 0.64) than in pH6.5 FaSSIF (with/without HPMCP-50 ratio in NTD concentration, 0.83). The reasons for these phenomena could be as follows. NTD was dissolved at higher concentrations in pH3.9 acetate buffer due to its higher solubility than in pH6.5 FaSSIF. On the other hand, HPMCP-50 is insoluble under acidic conditions, but soluble in neutral and basic aqueous vehicles (Home page of Shin-Etsu Chemical Co., Ltd.). Therefore, HPMCP-50 should be incorporated in the nanoemulsion droplets without being released in pH3.9 buffer, leading to the higher viscosity within the droplets. In contrast, HPMCP-50 would have been released from the nanoemulsion droplets due to its solubility in pH6.5 FaSSIF (Home page of Shin-Etsu Chemical Co., Ltd.), leading to relatively lower viscosity within the droplets.

Since we observed that pH3.9 buffer and pH6.5 FaSSIF became cloudy during the dissolution studies above, the particle sizes of nanoemulsion droplets diluted with distilled water, pH3.9 buffer, or pH6.5 FaSSIF were determined for NTD-CSA SNEDDS with or without 2% HPMCP-50 and compared with those for SNEDDS vehicle and 2% HPMCP-50 SNEDDS without NTD-CSA (Table 4). NTD-CSA increased the droplet sizes only in distilled water, but to a lesser extent. HPMCP-50 increased those in distilled water and pH3.9 acetate buffer, revealing that HPMCP-50 tended to increase droplet sizes more than NTD-CSA except in FaSSIF. Furthermore, it was found that the inclusion of both NTD-CSA and 2% HPMCP-50 unexpectedly resulted in very large sizes and pdi values in all the aqueous vehicles (Table 4). However, Figs. 6 and 7 indicated that NTD-CSA was almost completely dissolved in the filtrate through 0.45 μm filter and the concentrations of NTD dissolved directly in the aqueous phase of buffers were very low (Fig. 8), indicating that almost all of NTD-CSA should be incorporated into the nanoemulsion droplets and/or micelles less than 450 nm in diameter. Then, we confirmed that nanoemulsion droplets in the supernatant obtained after centrifuging the samples prepared for determining the particle size were smaller than those before centrifugation, also less than 450 nm (Table 4). Furthermore, 106.3 ± 5.3% (n = 3), 95.8 ± 1.7% (n = 3), and 87.7 ± 4.1% (n = 3) of NTD were recovered in the obtained supernatant for distilled water, acetate buffer, and pH6.5 FaSSIF, respectively. Although the recovery in pH6.5 FaSSIF was lower than others, NTD would have been precipitated following its release from nanoemulsion droplets, which might have been induced due to the release of HPMCP-50, soluble in pH6.5 FaSSIF, during the centrifugation. Therefore, we think that larger particles detected would be aggregates formed by HPMCP-50 itself, which were also observed in our previous study (Sumimoto et al., 2022). The details remain to be clarified, but NTD-CSA might have decreased the solubility of HPMCP-50 in SNEDDS vehicle and HPMCP-50 pushed out from the nanoemulsion droplets would have aggregated. This possibility suggests that formulation improvement should be needed in terms of HPMCP-50 contents and the components of SNEDDS vehicle.

3.6. *In vivo oral absorption study*

Finally, the in vivo performance has been examined for formulations

Table 4
Particle sizes of nanoemulsion droplets formed from 2% HPMCP-50 NTD-CSA SNEDDS.

Medium	Parameters	SNEDDS formulations				
		Vehicle only[§]	with NTD-CSA	with 2% HPMCP-50[§]	with NTD-CSA and 2% HPMCP-50	
					before centrifuged	after centrifuged
Distilled water	Particle size (nm)	40.45 ± 0.22	97.17 ± 19.23**	182.00 ± 6.72**	735.40 ± 54.16**	295.67 ± 17.92**
	Pdi	0.110 ± 0.013	0.833 ± 0.032**	0.655 ± 0.119**	0.993 ± 0.012**	0.833 ± 0.131**
pH3.9 acetate buffer	Particle size (nm)	49.10 ± 0.22	56.78 ± 0.11	255.20 ± 21.55**	730.73 ± 180.50**,††	62.34 ± 0.08
	Pdi	0.123 ± 0.012	0.370 ± 0.005**	0.540 ± 0.085**	0.908 ± 0.160**,††	0.404 ± 0.006**
pH6.5 FaSSIF	Particle size (nm)	44.65 ± 0.23	69.36 ± 0.52	64.82 ± 0.41	404.77 ± 83.65**,††	96.15 ± 2.81
	Pdi	0.113 ± 0.012	0.434 ± 0.007**	0.153 ± 0.010**	1.00 ± 0.00**,††	0.688 ± 0.03**

Results are expressed as the mean ± S.D. of three, six, or nine experiments. [§] cited from Sumimoto et al., 2022. Individual data were shown at supplementary Tables 1 and 2. **, $p < 0.01$ compared with SNEDDS vehicle in each medium. ††, $p < 0.01$ compared with each corresponding supernatant after centrifugation.

prepared for NTD including Ofev® (Fig. 9 and Table 5). Two% HPMCP-50 NTD-CSA SNEDDS provided significantly higher plasma concentrations and larger AUC compared with other preparations including Ofev® and NTD-CSA SNEDDS without HPMCP-50. Specifically, the AUC of NTD obtained by 2% HPMCP-50 NTD-CSA SNEDDS was significantly 1.52 times larger than that of Ofev®. Considering that the outcome of amorphous solid dispersion (Qin et al., 2022) or lipid carrier preparation (Zhu et al., 2020) would be equivalent or inferior to Ofev®, respectively, based on the reported values of AUC, 2% HPMCP-50 NTD-CSA SNEDDS would be more promising for improving NTD absorption. Furthermore, Fig. 9 (B) revealed that 2% HPMCP-50 NTD-CSA SNEDDS could reduce the inter-individual variation in oral absorption kinetics compared with Ofev®, which has been reported to cause a relatively large inter-individual variability (Wind et al., 2019). These results clearly indicated that the combination of co-amorphization with SNEDDS has been successful for the improvement of oral absorption behavior of NTD. On the other hand, NTD-CSA SNEDDS without HPMCP-50 preparation was almost equivalent to Ofev®, indicating the importance of HPMCP-50. Since HPMCP-50 can decrease the degree of supersaturation (Fig. 4) and has a viscous nature (Home page of Shin-etsu Chemical Co., Ltd.), the polymer would suppress the precipitation of NTD thermodynamically and kinetically (Brouwers et al., 2009; Xu and Dai, 2013) to some extent. However, we think that the suppression of drug release from nanoemulsion droplets (Fig. 8) would be the most important factor for HPMCP-50 to improve the oral absorption of NTD as discussed above.

Contribution of lymphatic transport to the absorption improvement of NTD by 2% HPMCP-50 NTD-CSA SNEDDS would not be so large since the solubility of NTD-CSA is only 21 μg/mL in olive oil and clogP is deduced to be similar to that of NTD-ESA (3.6, Table 1) (Sumimoto et al., 2022), which do not meet the pre-requisites for preferential lymphatic transport (over 50 mg/mL of solubility in triglyceride of long-chain fatty acid and over 5 of logP value) (Charman et al., 1986), and long-chain fatty acids facilitating lymphatic drug transport (Porter et al., 2008; Imada et al., 2015) were not used to prepare SNEDDS formulations in the current study.

On the other hand, the ratio of 2% HPMCP-50 NTD-CSA SNEDDS to Ofev® in AUC was 1.52 and the ratio to NTD-ESA powder was 3.58, which are too small considering the extensive improvement of NTD dissolution in pH6.5 FaSSIF by NTD-CSA SNEDDS preparations (Fig. 7 (A)). The differences that the in vivo study provided would likely come to be more moderate, compared with the differences observed in the in vitro studies (McEvoy et al., 2014), but the reasons for such a large discrepancy between in vitro and in vivo remain to be clarified.

Then, we have attempted to discuss the issue as follows:

(i) Reasons for oral absorption higher than expected for NTD-CSA, NTD-NSA powders; Very good dissolution of NTD in pH3.9 acetate buffer (Fig. 6 (A)) suggests that the "spontaneous supersaturation" (Brouwers et al., 2009) would have been formed after transferred to the small intestine, which would largely contribute to the absorption from the proximal regions of small intestine. In fact, it was reported that the oral absorption of atazanavir (Tomilo et al., 2006) or itraconazole (Lim et al., 1993; Willems et al., 2001) was dependent on the degree of spontaneous supersaturation.

(ii) Reasons for oral absorption lower than expected for SNEDDS formulations;

a) In contrast, the higher degree of supersaturation may lead to the lower BA as in the case of solid dispersion preparations of itraconazole (Six et al., 2005). In such a case, since the nucleation rate is highly dependent on the degree of supersaturation (Brouwers et al., 2009), the nucleation rates increased dependent on the extent of supersaturation might have been superior to the absorption rates of dissolved itraconazole emptied from the stomach. For the absorption rate to exceed the precipitation rate, therefore, it should still be important to maintain the supersaturation after transferred to the small intestine.

b) Taking into account of considerations above, the maintenance of supersaturation as observed in the in vitro dissolution study (Fig. 7 (A)) might not have occurred in vivo after oral dosing. In the current study, we performed the in vitro dissolution studies at constant acidic (pH3.9) or neutral condition (pH6.5), but some phenomena might have occurred only through a sequential exposure from the gastric to the small intestinal environments in vivo, i.e., i) possible changes in physicochemical properties of nanoemulsion droplets and/or lipoidal component forming nanoemulsion droplets, ii) subsequent changes in release properties of drugs from nanoemulsion droplets. iii) NTD dissolved directly in the aqueous phase at higher concentrations under acidic condition than those under neutral condition (Fig. 8) might have precipitated instead of being absorbed after transferred to the small intestine. iv) This precipitation might have also facilitated the nucleation of NTD newly released from nanoemulsion droplets and/or micelles.

c) "Nucleation in the gastrointestinal lumen will be facilitated by various surfaces and interfaces, only existing in vivo, that may act a catalyst for nucleation" (Brouwers et al., 2009). Some lipoidal components forming nanoemulsion droplets would be subjected to digestion and/or absorption (Mu et al., 2013), which would facilitate the release

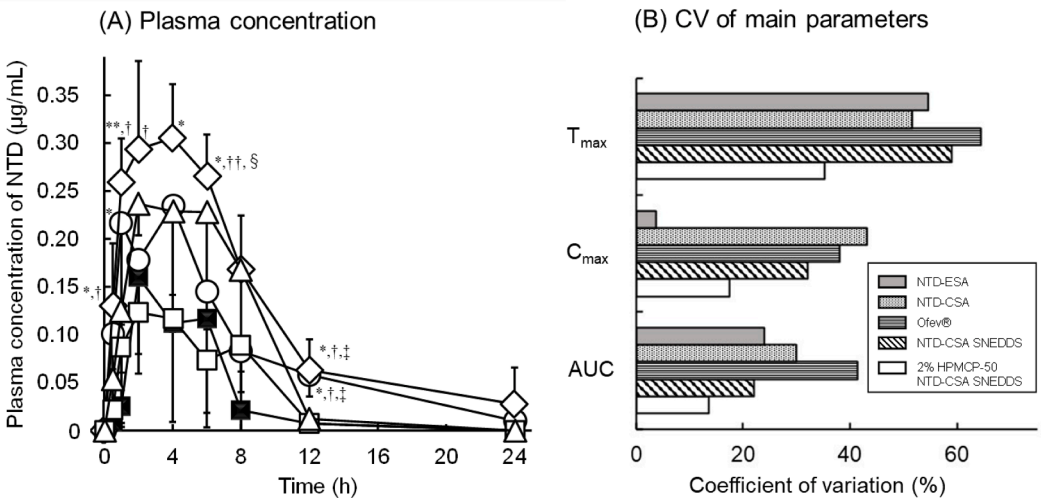

Fig. 9. In vivo oral absorption of NTD after dosing of NTD-CSA SNEDDS formulations to rats. (A) Plasma concentration – time profile. Results are expressed as the mean with S.D. bars of four to seven experiments. (B) Coefficient of variation for main pharmacokinetic parameters. **, $p < 0.01$; *, $p < 0.05$ compared with NTD-ESA powder. ††, $p < 0.01$; †, $p < 0.05$ compared with NTD-CSA powder. ‡, $p < 0.05$ compared with Ofev®. §, $p < 0.05$ compared with NTD-CSA SNEDDS. Keys: ■, NTD-ESA powder; □, NTD-CSA powder; △, Ofev®; ○, NTD-CSA SNEDDS; ◇, 2% HPMCP-50 NTD-CSA SNEDDS.

Table 5
Pharmacokinetic parameters of NTD after oral administration of SNEDDS formulations of NTD-CSA.

Formulations	T_{max} (h)	C_{max} (μg/mL)	AUC (μg/mL·h)	Ratio to NTD-ESA in AUC	Ratio to Ofev® in AUC
NTD-ESA powder	3.50 ± 1.91	0.23 ± 0.01	0.84 ± 0.20	–	0.42
NTD-CSA powder	5.00 ± 2.58	0.12 ± 0.05	0.97 ± 0.29	1.15	0.49
Ofev®	4.60 ± 2.97	0.22 ± 0.09	1.99 ± 0.82*,†	2.36	–
NTD-CSA SNEDDS	2.71 ± 1.60	0.31 ± 0.10††	2.01 ± 0.44**,†	2.39	1.01
2% HPMCP-50 NTD-CSA SNEDDS	4.00 ± 1.41	0.36 ± 0.06††	3.02 ± 0.41**,††,‡,§	3.58	1.52

T_{max} and C_{max} were observed values. AUC was calculated from 0 to 24 h by the trapezoidal rule. Dose of NTD was 30 mg/kg. Results are expressed as the mean ± S.D. of four to seven experiments except for the ratio in AUC. Individual data were shown at supplementary Tables 3, 4, and 5. **, $p < 0.01$; *, $p < 0.05$ compared with NTD-ESA. ††, $p < 0.01$; †, $p < 0.05$ compared with NTD-CSA. ‡, $p < 0.05$ compared with Ofev®. §, $p < 0.05$ compared with NTD-CSA SNEDDS.

of drugs from nanoemulsion droplets.

We have planned and are performing several experiments to find out the reasons for causing such a large discrepancy between in vitro and in vivo performances, and to further improve the oral absorption behavior of NTD.

4. Conclusion

By using CSA as a counter ion, the high crystallinity of NTD-ESA was disrupted and NTD was successfully co-amorphized with CSA to form NTD-CSA. Furthermore, the SNEDDS formulation of NTD-CSA with 2 % HPMCP-50 greatly enhanced NTD dissolution under the small intestinal luminal conditions, and significantly outperformed Ofev® in the in vivo oral absorption of NTD. For further improvement of NTD absorption, the reasons for the large discrepancy between in vitro and in vivo performances should be clarified.

CRediT authorship contribution statement

Tomoya Inoue: Methodology, Investigation, Formal analysis. **Seito Maehara:** Investigation, Formal analysis. **Masato Maruyama:** Data curation. **Kazutaka Higaki:** Writing – review & editing, Writing – original draft, Visualization, Supervision, Methodology, Conceptualization.

Declaration of competing interest

The authors declare that they have no known competing financial interests or personal relationships that could have appeared to influence the work reported in this paper.

Data availability

Data will be made available on request.

Appendix A. Supplementary material

Supplementary data to this article can be found online at https://doi.org/10.1016/j.ijpharm.2024.124197.

References

Aikawa, S., Tanaka, H., Ueda, H., Maruyama, M., Higaki, K., 2023. Formation of a stable co-amorphous system for a brick dust molecule by utilizing sodium taurocholate with high glass transition temperature. Pharmaceutics 15, 84.

Bergstrom, C.A.S., Charman, W.N., Porter, C.J.H., 2016. Computational prediction of formulation strategies for beyond-rule-of-5 compounds. Adv. Drug Deliv. Rev. 101, 6–21.

Brouwers, J., Brewster, M.E., Augustijns, P., 2009. Supersatrurating drug delivery systems: The answer to solubility-limited oral bioavailability? J. Pharm. Sci. 98, 2549–2572.

Charman, W.N., Stella, V.J., 1986. Estimating the maximal potential for intestinal lymphatic transport of lipophilic drug molecules. Int. J. Pharm. 34, 175–178.

Chougule, M., Sirvi, A., Saini, V., Kashyap, M., Sangamwar, A.T., 2023. Enhanced biopharmaceutical performance of brick dust molecule nilotinib via stabilized amorphous nanosuspension using a facile acid-base neutralization approach. Drug Deliv. Transl. Res. 13, 2503–2519.

Dallinger, C., Trommeshauser, D., Marzin, K., Liesener, A., Kaiser, R., Stopfer, P., 2016. Pharmacokinetic properties of nintedanib in healthy volunteers and patients with advanced cancer. J. Clin. Pharmacol. 56, 1387–1394.

Egorova, K.S., Gordeev, E.G., Ananikov, V.P., 2017. Biological activity of ionic liquids and their application in pharmaceutics and medicine. Chem. Rev. 117, 7132–7189.

FDA. Guidance for industry: estimating the maximum safe starting dose in initial clinical trials for therapeutics in adult healthy volunteers 2005. https://www.fda.gov/regulatory-information/search-fda-guidance-documents/estimating-maximum-safe-starting-dose-initial-clinical-trials-therapeutics-adult-healthy-volunteers.

Hawley, M., Morozowich, W., 2010. Modifying the diffusion layer of soluble salts of poorly soluble basic drugs to improve dissolution performance. Mol. Pharm. 7, 1441–1449.

Hiew, T.N., Zemlyanov, D.Y., Taylor, L.S., 2022. Balancing solid-state stability and dissolution performance of lumefantrine amorphous solid dispersions: The role of polymer choice and drug-polymer interactions. Mol. Pharm. 19, 392–413.

Hilberg, F., Roth, G.J., Krssak, M., Kautschitsch, S., Sommergruber, W., Tontsch-Grunt, U., Garin-Chesa, P., Bader, G., Zoephel, A., Quant, J., Heckel, A., Rettig, W.J., 2008. BIBF 1120: Triple angiokinase inhibitor with sustained receptor blockade and good antitumor efficacy. Cancer Res. 68, 4774–4782.

Holm, R., Kuentz, M., Ilie-Spiridon, A.-R., Griffin, B.T., 2023. Lipid based formulations as supersaturating oral delivery systems: From current to future industrial applications. Eur. J. Pharm. Sci. 189, 106556.

Home page of Shin-Etsu Chemical Co., Ltd. https://www.metolose.jp/en/ pharmaceutical/.

Huang, J., Chen, P.X., Rogers, M.A., Wettig, S.D., 2019. Investigating the phospholipid effect on the bioaccessibility of rosmarinic acid-phospholipid complex through a dynamic gastrointestinal in vitro model. Pharmaceutics 11, 156.

Imada, C., Takahashi, T., Kuramoto, M., Masuda, K., Ogawara, K., Sato, A., Wataya, Y., Kim, H.-S., Higaki, K., 2015. Improvement of oral bioavailability of N-251, a novel antimalarial drug, by increasing lymphatic transport with long-chain fatty acid-based self-nanoemulsifying drug delivery system. Pharm. Res. 32, 2595–2608.

Ishikawa, M., Hashimoto, Y., 2011. Improvement in aqueous solubility in small molecule drug discovery programs by disruption of molecular planarity and symmetry. J. Med. Chem. 54, 1539–1554.

Jadhav, K., Sirvi, A., Janjal, A., Kashyap, M.C., Sangamwar, A.T., 2024. Utilization of lipophilic salt and phospholipid complex in lipid-based formulations modulate drug loading and oral bioavailability of pazopanib. AAPS PharmSciTech 25, 59.

Kasten, G., Löbmann, K., Grohganz, H., Rades, T., 2019. Co-former selection for co-amorphous drug-amino acid formations. Int. J. Pharm. 557, 366–373.

Koehl, N.J., Holm, R., Kuentz, M., Griffine, B.T., 2019. New insights into using lipid based suspensions for 'brick dust' molecules: case study of nilotinib. Pharm. Res. 36, 56.

Koehl, N.J., Holm, R., Kuentz, M., Griffine, B.T., 2020. Chase dosing of lipid formulations to enhance oral bioavailability of nilotinib in rats. Pharm. Res. 37, 124.

Lale, A.S., Sirvi, A., Debafe, S., Patil, S., Sangamwar, A.T., 2024. Supersaturable diacyl phospholipid dispersion for improving oral bioavailability of brick dust molecule: a case study of aprepitant. Eur. J. Pharm. Biopharm. Apr:197:114241.doi:10.1016/ j.ejpb.2024.114241. Epub 2024 Mar 1.

Lim, S.G., Sawyerr, A.M., Hudson, M., Sercombe, J., Pounder, R.E., 1993. Short report: The absorption of fluconazole and itraconazole under conditions of low intragastric acidity. Aliment Pharmacol. Ther. 7, 317–321.

Luedtke, D., Marzin, K., Jungnik, A., von Wangenheim, U., Dallinger, C., 2018. Effects of ketoconazole and rifampicin on the pharmacokinetics of nintedanib in healthy subjects. Eur. J. Drug Metab. Pharmacokinet. 43, 533–541.

McConnell, E.L., Basit, A.W., Murdan, S., 2008. Measurements of rat and mouse gastrointestinal pH, fluid and lymphoid tissue, and implications for in-vivo experiments. J. Pharm. Pharmacol. 60, 63–70.

McEvoy, C.L., Trevaskis, N.L., Edwards, G.A., Perlman, M.E., Ambler, C.M., Mack, M.C., Brockhurst, B., Porter, C.J.H., 2014. In vitro-in vivo evaluation of lipid based formulations of the CETP inhibitors CP-529,414 (torcetrapib) and CP-532,623. Eur. J. Pharm. Biopharm. 88, 973–985.

Meola, T.R., Dening, T.J., Prestidge, C.A., 2018. Nanocrystal-silica-lipid hybrid particles for the improved oral delivery of ziprasidone in vitro. Eur. J. Pharm. Biopharm. 129, 145–153.

Morgen, M., Szxena, A., Chen, X.-Q., Miller, W., Nkansah, R., Goodwin, A., Cape, J., Haskell, R., Su, C., Gudmundsson, O., Hageman, M., Kumar, A., Chowan, G.S., Rao, A., Holenarsipur, V.K., 2017. Lipophilic salts of poorly soluble compounds to enable high-dose lipidic SEDDS formulations in drug discovery. Eur. J. Pharm. Biopharm. 117, 212–223.

Mu, H., Holm, R., Müllertz, A., 2013. Lipid-based formulations for oral administration of poorly water-soluble drugs. Int. J. Pharm. 453, 215–224.

NDA review, FDA Center for Drug Evaluation and Research. Nintedanib pharmacology, Feb 2014. chrome-extension://efaidnbmnnnibpcajpcglclefindmkaj/https://www.accessdata.fda.gov/drugsatfda_docs/nda/2014/205832Orig1s000PharmR.pdf. Accessed 9 June 2023.

Nora, G.-I., Venkatasubramanian, R., Strindberg, S., Siqueira-Jorgensen, S.D., Pagano, L., Romanski, F.S., Swarnakar, N.K., Rades, T., Müllertz, A., 2022. Combining lipid based drug delivery and amorphous solid dispersions for improved oral drug absorption of poorly water-soluble drug. J. Controlled Rel. 349, 206–212.

Nyamba, I., Lechanteur, A., Bemdé, R., Evrard, B., 2021. Physical formulation approaches for improving aqueous solubility and bioavailability of ellagic acid: a review. Eur. J. Pharm. Biopharm. 159, 198–210.

Okawa, S., Sumimoto, Y., Masuda, K., Ogawara, K., Maruyama, M., Higaki, K., 2021. Improvement of lipid solubility and oral bioavailability of a poorly water-soluble and poorly lipid-soluble drug, rebamipide, by utilizing its counter ion and SNEDDS preparation. Eur. J. Pharm. Sci. 159, 105721.

Package insert of Ofev®, 2022, Boehringer Ingelheim. OFEV® (nintedanib) capsules, for oral use [package insert]. Ridgefield: Boehringer Ingelheim Pharmaceuticals; 2022. chrome-xtension://efaidnbmnnnibpcajpcglclefindmkaj/https://content. boehringer-ingelheim.com/DAM/b5d67da8-329b-4fa4-a732-af1e011fc0a5/ofev-us-pi.pdf. Accessed 9 June 2023.

Porter, C.J.H., Pouton, C.W., Cuine, J.F., Charman, W.N., 2008. Enhancing intestinal drug solubilisation using lipid-based delivery systems. Adv. Drug Deliv. Rev. 60, 673–691.

Qin, Y., Xiao, C., Li, X., Huang, J., Si, L., Sun, M., 2022. Enteric polymer-based amorphous solid dispersions enhance oral absorption of the weakly basic drug Nintedanib via stabilization of supersaturation. Pharmaceutics. 14, 1830.

Roth, G.J., Binder, R., Colbatzky, F., Dallinger C., S-Herceg, R., Hilberg, F., Wollin, S-L., Kaiser, R., 2015. Nintedanib; From discovery to the clinic. J. Med. Chem. 58, 1053-1063.

Roth, G.J., Heckel, A., Colbatzky, F., Handschuh, S., Kley, J., Lehmann-Lintz, T., Ralf Lotz, R., Tontsch-Grunt, U., Walter, R., Hilberg, F., 2009. Design, synthesis, and evaluation of indolinones as triple angiokinase inhibitors and the discovery of a highly specific 6-methoxycarbonyl-substituted indolinone (BIBF 1120). J. Med. Chem. 52, 4466–4480.

Sahbaz, Y., Williams, H.D., Nguyen, T.-H., Saunders, J., Ford, L., Charman, S.A., Scammells, P.J., Porter, C.J.H., 2015. Transformation of poorly water-soluble drugs into lipophilic ionic liquids enhances oral drug exposure from lipid based formulations. Mol. Pharm. 12, 1980–1991.

Sahbaz, Y., Nguyen, T.-H., Ford, L., McEvoy, C.L., Williams, H.D., Scammells, P.J., Porter, C.J.H., 2017. Ionic liquid forms of weakly acidic drugs in oral lipid formulations: Preparation, characterization, in vitro digestion, and in vivo absorption studies. Mol. Pharm. 14, 3669–3683.

Serajuddin, A.T.M., 1999. Solid dispersion of poorly water-soluble drugs: Early promises, subsequent problems, and recent breakthroughs. J. Pharm. Sci. 88, 1058–1066.

Six, K., Daems, T., de Hoon, J., Van Hecken, A., Depre, M., Bouche, M., Prinsen, P., Verreck, G., Peeters, J., Brewster, M.E., Van den Mooter, G., 2005. Clinical study of solid dispersions of itraconazole prepared by hotstage extrusion. Eur. J. Pharm. Sci. 24, 179–186.

Stella, V.J., Nti-Addae, K.W., 2007. Prodrug strategies to overcome poor water solubility. Adv. Drug Del. Rev. 59, 677–694.

Sumimoto, Y., Okawa, S., Inoue, Y., Masuda, K., Maruyama, M., Higaki, K., 2022. Extensive improvement of oral bioavailability of mebendazole, a brick dust, by polymer-containing SNEDDS preparation: Disruption of high crystallinity by utilizing its counter ion. Eur. J. Pharm. Biopharm. 172, 213–227.

Summary of product characteristics. Ofev. European Medicines Agency.26 Nov 2018. chrome-extension://efaidnbmnnnibpcajpcglclefindmkaj/https://www.ema.europa.eu/ documents/product-information/ofev-epar-product-information_en.pdf. Accessed 9 June 2023.

Tomilo, D.L., Smith, P.F., Ogundele, A.B., Difrancesco, R., Berenson, C.S., Eberhardt, E., Bednarczyk, E., Morse, G.D., 2006. Inhibition of atazanavir oral absorption by lansoprazole gastric acid suppression in healthy volunteers. Pharmacother. 26, 341–346.

Willems, L., van der Geest, R., de Beule, K., 2001. Itraconazole oral solution and intravenous formulations: a review of pharmacokinetics and pharmacodynamics. J. Clin. Pharm. Ther. 26, 159–169.

Wind, S., Schmid, U., Freiwald, M., Marzin, K., Lotz, R., Ebner, T., Stopfer, P., Dallinger, C., 2019. Clinical pharmacokinetics and pharmacodynamics of Nintedanib. Clin. Pharmacokinet. 58, 1131–1147.

Xu, S., Dai, W.-G., 2013. Drug precipitation inhibitors in supersaturable formulations. Int. J. Pharm. 453, 36–43.

Yamashita, T., Ozaki, S., Kushida, I., 2011. Solvent shift method for anti-precipitant screening of poorly soluble drugs using biorelevant medium and dimethyl sulfoxide. Int. J. Pharm. 419, 170–174.

Zhu, Y., Liang, X., Lu, C., Kong, Y., Tang, X., Zhang, Y., Yin, T., Gou, J., Wang, Y., He, H., 2020. Nanostructured lipid carriers as oral delivery systems for improving oral bioavailability of nintedanib by promoting intestinal absorption. Int. J. Pharm. 586, 119569.